Volume 10, Number 1, 2017. pp. 17-22

Jordan Journal of Physics

ARTICLE

Free Breathing Abdominal Imaging with Fat-Water Separation Using 3D Radial Stack-of-Stars Trajectory

Riad S. Ababneh

Physics Department, Yarmouk University, Irbid: 21163, Jordan.

Received on: 21/8/2016; *Accepted on: 3/1/2017*

Abstract: In earlier studies of fat-water separation using dynamic imaging applications, the three-dimensional (3D) MRI failed to provide high spatial and temporal resolution. This work proposes a fat-water separation strategy in the abdomen during free breathing using the 3D stack-of-stars (SOS) radial sampling technique. Radial trajectories are less sensitive to motion and have a higher sampling density for the central k-space, allowing for better performance in capturing dynamic information. To this end, a 3D radial TrueFISP sequence was modified to enable the echo time TE to change from projection to projection, where all z-phase encoding was acquired at a single projection angle before switching to the next projection angle. As a result, the fat signal is forced to behave in a specific and easily recognizable fashion over time. Using temporal processing, temporal variations imposed on fat signals can be recognized and fat signals can be separated from water signals.

Keywords: Fat-water separation, TrueFISP, Stack-of-stars, Free breathing.

Introduction

Using the 3D MRI to perform dynamic imaging of the abdomen is difficult due to the inevitable trade-off between temporal and spatial resolution and total acquisition time. Several methods have been proposed to improve temporal resolution and spatial resolution. Examples include view sharing [1], keyhole imaging [2] and the 3D TRICKS [3] method.

A non-Cartesian acquisition of k-space was widely accepted as a potentially superior alternative to the 3D MRI, due to its efficient use of MR gradient hardware and the fact that it is less affected by motion. The most prominent examples are radial trajectories and spiral trajectories. It is considerably more difficult to reconstruct [4] images of non-Cartesian trajectories, because the data points do not fall on a grid in k-space. There are many techniques for reconstructing the non-Cartesian data; for example, using the regularization and estimation theory [5], sampling density compensation in the MRI [6] and applying the non-uniform fast Fourier transformation (NUFFT) [7] (which is used in this manuscript to reconstruct the data).

Recently, the 3D radial stack-of-stars concept was introduced to reduce the total amount of sampled space and to provide short data acquisition times with high quality images [22]. The 3D k-space with a radial trajectory (using cylindrical sampling) is under-sampled in Fourier space. This trajectory (Fig. 1) is used for dynamic and motion sensitive imaging.

The magnetic resonance signals from fat and water differ slightly in frequency, making it possible to generate images of the places where these two types of tissues separate [8-10]. In applications where fat tends to obscure the pathology or where the disease itself has to do with adipose tissues, this ability can prove very valuable. These approaches, however, are ill-adapted to dynamic applications where temporal resolution is important, because they typically

Corresponding Author: R. S. Ababneh **Email**: riada@yu.edu.jo

require lengthy acquisition of three or more separate images with different imaging parameters to allow robust fat-water separation in the presence of magnetic field inhomogeneities.

Radial MRI techniques have gained increasing attention in dynamic imaging and have been successfully used in many applications, such as cardiac imaging [11-14] and abdominal imaging [15-16]. Radial MRI data is sampled using the golden-angle scheme, where the angle of the radial lines is increased continuously by 111.25°, giving a higher sampling density for the central k-space and higher spatial and temporal resolutions. The basic property of this angle is that each successive view divides the largest remaining angular gap and this process continues *ad infinitum*. As a result, the k-space will be approximately uniformly sampled for any number of views chosen for reconstruction. The radial MRI does not detect object motion during data acquisition [17-18], which improves its ability to capture dynamic information. Consequently, more 3D gradient sequences have been developed (radial TrueFISP) that use the stack-of-stars technique to acquire volumetric k-space data. Images acquired during free breathing examinations using the stack-of-stars radial TrueFISP sequence are often of a higher quality than those acquired during conventional examinations where the patient holds his/her breath [19-21].

This project focused on robust volumetric fat-water separation in the presence of respiratory motion using a 3D radial imaging technique. Existing methodology cannot achieve high-resolution volumetric fat-water separation during a breath-hold exam. While a single volume can be acquired in one held breath, the need to acquire three images for each volume hampers fat-water separation in the abdomen. Therefore, this project was targeted towards developing strategies for the acquisition of 3D volumes to allow robust fat-water separation in the presence of respiratory motion; thus, the stack-of-stars concept has the potential to improve temporal resolution. This approach was implemented and both phantom and volunteer results are presented in the findings.

Materials and Methods

The 3D radial TrueFISP pulse sequence was modified to include radial stack-of-stars k-space sampling in the xy-plane and Cartesian encoding in the z direction. In this sequence, all partitions corresponding to the first radial angle were acquired sequentially before moving to the next angle (see Fig. 1). For angular ordering, the sequence used the golden-angle scheme, where the angle is increased each time by $G_{\Phi}=111.25^{o}$, which corresponds to 180^{o} multiplied by the golden ratio [23].

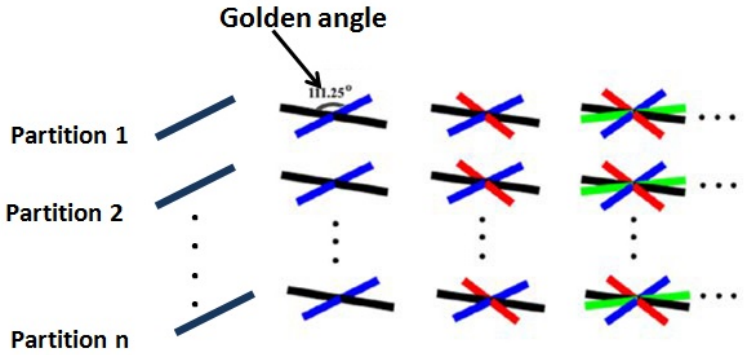

FIG. 1. The stack-of-stars sampling.

The sequence developments were done on IDEA (the SIEMENS sequence development software) and implemented on a clinical 3.0T MRI scanner (SIEMENS Magnetom SKYRA). The development started with the 2D radial bSSFP (Balanced Steady-state free precession) sequence. To that end, a standard Cartesian Gradient Echo (GE) sequence was modified to build a bSSFP sequence by refocusing all imaging gradients between subsequent excitation radio frequency pulses. A variable delay was inserted before and after each excitation pulse to allow for variable echo times (TE) at constant repetition times (TR). In addition, the frequency

response function was shifted to on-resonance frequency by applying alternating RF-pulse phases (0°-180°). In the last step, a flip angle ramp and dummy pulses were added to the sequence to minimize oscillations and allow the magnetization to reach steady state. The sequence was extended to allow for a radial acquisition scheme following a quasi-random order of the radial projections. The single-slice sequence described above was extended to allow for volumetric acquisition and respiratory self-gating, by implementing 3D encoding gradient tables and a DC navigator signal after refocusing all imaging gradients. The sequence was validated and tested on phantoms containing different tubes filled with water and oil.

Fig. 2. shows the schematic of the modified sequence allowing for variable echo times (TE) at constant repetition time (TR). In this sequence, TE was made to vary between subsequent spokes. Specifically, a series of 3 TEs was employed and periodically repeated following a radial golden angle projection order, thereby distributing the acquired fat signal over the temporal frequency domain. The 3D sequence allows for in-plane radial sampling with arbitrary sampling orders. Fig. 2B illustrates the stack-of-stars trajectory, where the angles of the radial spokes are ordered using the golden-angle scheme. The kx-ky plane was acquired along radial spokes and with Cartesian sampling along the kz plane. The sequence was implemented in standard mode – where the echo-time is shifted from image to image – and in interleaved mode – where echo time is varied from line to line (i.e., projection to projection). In addition, a DC navigator signal is acquired after balancing all imaging gradients. This signal can be used for respiratory gating.

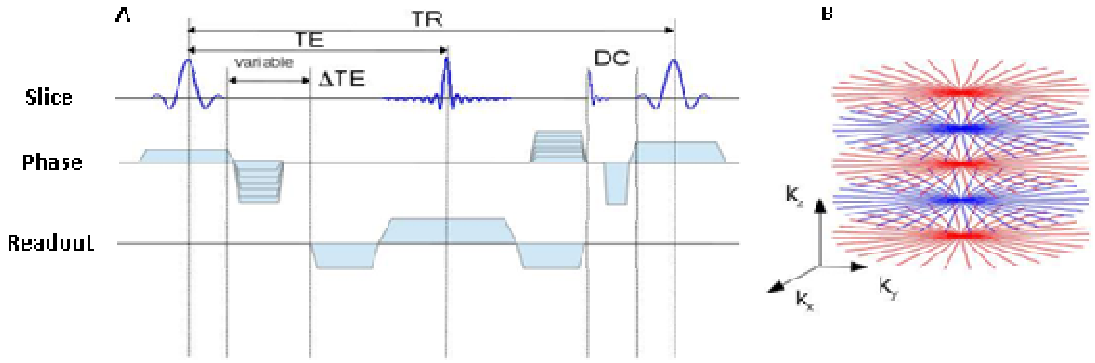

FIG. 2. (A) Schematic of the modified bSSFP sequence allowing for variable echo times (TE) at constant repetition time (TR). The 3D sequence allows for in-plane radial sampling with arbitrary sampling orders. The sequence has been implemented in standard mode, where the echo-time is shifted from image to image and in interleaved mode, where echo time is varied from line to line (i.e., projection to projection). In addition, a DC navigator signal is acquired after balancing all imaging gradients. This signal can be used for respiratory gating. (B) The k-space trajectory following a stack-of-stars trajectory.

The data is acquired by sampling all lines for the first golden angle in all partitions (all phase-encoding steps along the SLICE direction), then sampling all lines with the second golden angle (Fig. 1). This technique preserved the motion robustness of radial sampling and reduced the motion sensitivity, which leads to high data consistency within the spoke stacks.

Experiments were carried out on a 3.0T clinical scanner using the following imaging parameters: Number of projections =1500, number of partition = 28, TR = 4.0 ms, flip angle = 40°, FOV= 400x400 mm^2, radial readout points = 256 and TEs of TE_1 = 1.6, TE_2 = 2.0 and TE_3 = 2.4 ms. Signals within each partition were used to generate images at different TEs using non-uniform fast Fourier transform (NUFFT) gridding [7]. Finally, according to Ababneh et al. [22], fat-water separation was captured frame-by-frame and separation was achieved for all reconstructed partitions. All the acquired data was reconstructed offline using a MatLab software package (Math Works, Natick, MA). In this work, we integrated the fat-water separation method used in [22] with the 3D radial stack-of-stars technique during free-breathing abdominal imaging. Results were obtained *in-vivo* at 3T for the abdomen.

Results

The experiments were performed on a 3.0T clinical MRI scanner (Siemens, Erlangen, Germany) using a 32 spinal coil positioned around the mid-portion of the body and body array, by employing the modified 3D radial TrueFISP pulse sequence. Fig. 1 shows the stack-of-stars sampling pattern, where data is acquired by sampling all lines for the first golden angle in all partitions, then the second lines, … and so on. The spokes are approximately uniformly distributed and each spoke represents one readout.

Fig. 2A is the schematic diagram of the modified sequence used in this work and Fig. 2B illustrates all of the partitions in the stack-of-stars technique.

Phantoms are simple tools used to evaluate imaging experiments. They are important, because they provide reproducible and accurate results and offer a convenient test bed for developments related to *in-vivo* imaging. The phantom contains two tubes with water and oil to provide a fat signal. Fig. 3 depicts a single time frame on a 3T clinical MRI scanner acquired with the static phantom containing water and oil (fat). Calculated water and fat images are also shown.

Fig. 4 shows one image acquired at 3T with a healthy volunteer, where both fat and water are clear before the separation process. Fig. 5 shows calculated fat and water data acquired for one partition on a healthy volunteer. Water-only and fat-only results from one phase (out of 4) are shown in (a) and (b), respectively.

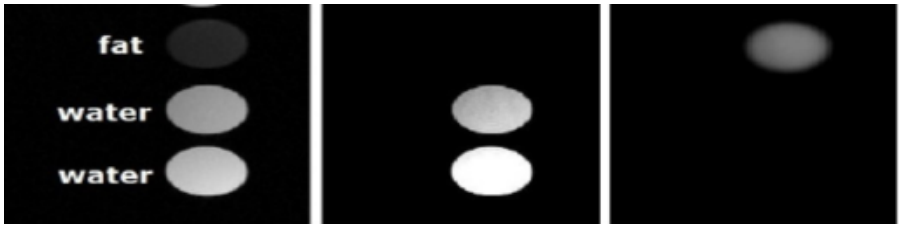

FIG. 3. Phantom experiments. Separation of multiple species (water and fat) out of one experiment with dynamic change of echo time from projection to projection. The method allows for perfect discrimination of the two species.

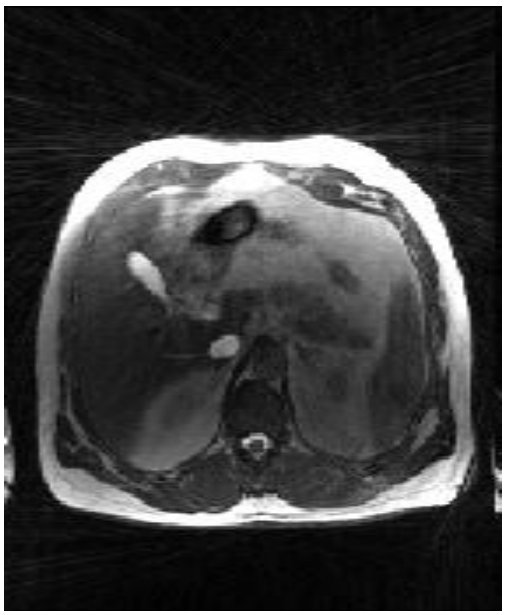

FIG. 4. One image acquired at 3T with a healthy volunteer, showing both fat and water before the separation process.

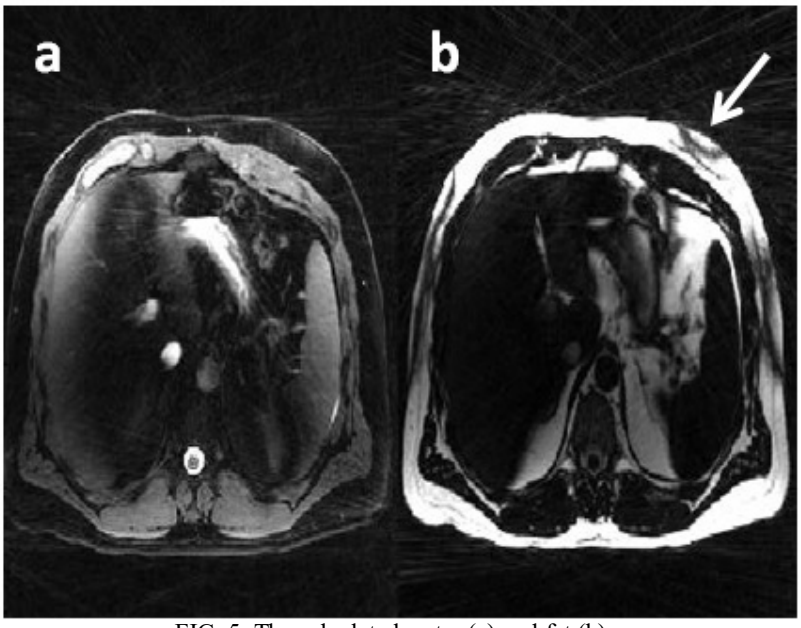

FIG. 5. The calculated water (a) and fat (b).

Discussion and Conclusion

This study presented a robust approach to separate fat and water signals using stack-of-stars 3D radial acquisition combined with non-uniform fast Fourier transform (NUFFT) gridding of different respiratory phases in free breathing. This technique reduces blurring artifacts caused by respiratory motion and enhances the image resolution. Compared to a 3D Cartesian acquisition and Dixon-RAVE [25-27], fat-water separation for free breathing abdominal imaging using 3D SOS has given promising results. Also, to show the advantage of this approach, abdominal imaging was performed in a healthy volunteer while the motion artifacts are inherently reduced. In terms of volume coverage, using the three-dimensional (3D) stack-of-stars trajectory might be advantageous compared to 2D techniques.

Phantom experiments were used, especially at the beginning of the project, to confirm a successful pulse sequence development and to validate the method used to separate fat and water. The images in Fig. 3 show an excellent separation of the two components in the static water-oil phantom.

This paper demonstrated the feasibility of 3D free breathing abdominal imaging using stack-of-stars trajectory. The phantom studies were performed to show that execution of the sequence is a function of golden angle and to evaluate imaging experiments.

The images suffer from banding artifacts due to off-resonance effects, which could be minimized through the use of one of the known methods. Our study results indicate that 3D TrueFISP with radial acquisition during free breathing is feasible for abdominal MRI studies. The results also demonstrate that even small variations in TE (0.4 ms) were sufficient to separate fat and water in dynamic objects. In conclusion, the approach was tested in time-resolved abdominal imaging. Good separation without streaking artifacts or blurring due to respiratory motion was obtained in all studied cases. The concept has been demonstrated in 3D. The 3D radial stack-of-stars TrueFISP sequence was modified by changing the echo time TE from projection to projection, to force fat signals to behave in a conspicuous manner over time, so that they can be detected and separated from water signals through temporal processing.

The radial stack-of-stars k-space trajectory is ideally suited for free breathing imaging, because it can tolerate motion better than conventional Cartesian trajectories. A major pitfall of 3D radial stack-of-stars TrueFISP imaging is its high sensitivity to magnetic field inhomogeneities (off-resonances). This could potentially lead to signal voids and unsuccessful fat-water separation. In 2D techniques, these artifacts can be minimized or avoided by appropriate shimming of the magnetic field

within the slice of interest. However, appropriate shimming of a larger volume (such as in 3D) is much more difficult to achieve. The resulting banding artifacts are clearly visible in all slices and are indicated by the white arrow in Fig. 3.

In conclusion, this study demonstrated that the 3D radial stack-of-stars TrueFISP imaging approach can be used to obtain high spatial and temporal resolutions for free breathing abdominal imaging. Moreover, it could be a promising approach for clinical imaging applications that require fat-water separation of different respiratory phases in free breathing. Future work will focus on applying the method to self-gated 3D radial imaging for robust fat-water separation in the abdomen.

Acknowledgements

Thanks are due to the Deutsche Forschungsgemeinschaft DFG BR 4356/2-1 for funding, as well as to SIEMENS, Healthcare Sector, Erlangen, Germany.

Fat-water-separated DCE imaging with high temporal and spatial resolution is possible with DCE-Dixon-RAVE. The Dixon-RAVE framework promises high value for clinical imaging applications that require fat/water separation.

References:

[1] Riederer, S.J., Tasciyan, T., Farzaneh, F., Lee, J.N., Wright, R.C. and Herfkens, R.J., Magn. Reson. Med., 8 (1988) 1.

[2] Vaals, J.J., Brummer, M.E., Dixon, W.T. et al., J. Magn. Reson. Imaging, 3 (1993) 671.

[3] Glover et al., MRM, 18 (1991) 371.

[4] Seiberlich, N., Ehses, P., Duerk, J., Gilkeson, R. and Griswold, M., Magn. Reson. Med., 65(2) (2011) 492.

[5] Rosenfeld, D., Magn. Reson. Med., 48(1) (2002) 193.

[6] Pipe, J.G. and Menon, P., Magn. Reson. Med., 41(1) (1999) 179.

[7] Fessler, J., IEEE Trans. Med., 51(2) (2003) 560.

[8] Xiang et al., JMRI, 7 (1997) 1002.

[9] Reeder et al., MRM, 51 (2004) 35.

[10] Glover, G.H. and Schneider, E., Magn. Reson. Med., 18 (1991) 371.

[11] Larson, A.C. and Simonetti, O.P., Magn. Reson. Med., 46 (2001) 1059.

[12] Schaeffter, R., Weiss, S., Eggers, H. and Rasche, V., Magn. Reson. Med., 46 (2001) 1238.

[13] Peters, D.C., Epstein, F.H. and McVeigh, E.R., Magn. Reson. Med., 45 (2001) 562.

[14] Barger, A.V., Grist, R.M., Block, W.F. and Mistretta, C.A., Magn. Reson. Med., 44 (2000) 821.

[15] Glover, G.H. and Pauly, J.M., Magn. Reson. Med., 28 (1992) 275.

[16] Altbach, M.I., Outwater, E.K., Trouard, T.P., Krupinski, E.A., Theilmann, R.J., Stopeck, A.T., Kono, M. and Gmitro, A.F., J. Magn. Reson. Imaging, 16 (2002) 179.

[17] Katoh, M., Spuentrup, E., Buecker, A., Manning, W.J., Guenther, R.W. and Botnar, R.M., J. Magn. Reson. Imaging, 23 (2006) 757.

[18] Trouard, T.P., Sabharwal, Y., Altbach, M.I. and Gmitro, A.F., J. Magn. Reson. Imaging, 6 (1996) 925.

[19] Chandarana, H., Block, T.K., Rosenkrantz, A.B. et al., Invest. Radiol., 46 (2011) 648.

[20] Azevedo, R.M., de Campos, R.O., Ramalho, M. et al., AJR Am. J. Roentgenol., 197 (2011) 650.

[21] Chen, L., Adluru, G., Schabel, M.C., McGann, C.J. and Dibella, E.V., Med. Phys., 39(8) (2012) 5204.

[22] Ababneh, R.S., Madore, B. and Jing, JMRI, 32 (2010) 962.

[23] Winkelmann, S., Schaeffter, T., Koehler, T., Eggers, H. and Doessel, O., IEEE T. Med. Imaging, 26 (2007) 68.

[24] Kai, T.B., Hersh, C., Sarah, M., Mary, B., Tom, M., Girish, F., Mari, H., Robert, G., Christian, G., Berthold, K. and Daniel K., JKSMRM, 18(2) (2014) 87.

[25] Thomas, B., Li, F., Daniel, K.S., Hersh, C. and Kai, T., Magn. Reson. Med., 76(3) (2016) 1522.

[26] Ababneh, R.S., Benkertb, T. and Breuerb, F., Jordan J. Phys., 9(2) (2016) 103.

[27] Chen, L., Adluru, G., Edward, M. and Dibella, V., Med. Phys., 39(8) (2012) 5204.